

1 Interleukin 11 therapy causes acute heart failure and its 2 use in patients should be reconsidered

3 Mark Sweeney MB BChir^{1,2,3}, Katie O’Fee MRes^{1,2}, Chelsie Villanueva-Hayes MSc^{1,2}, Ekhlas
4 Rahman MSc^{1,2}, Michael Lee PhD⁴, Henrike Maatz PhD^{5,6}, Eric L. Lindberg PhD⁵,
5 Konstantinos Vanezis PhD^{1,2,4}, Ivan Andrew BSc^{1,2}, Emma R. Jennings², Wei-Wen Lim
6 PhD^{7,8}, Anissa A Widjaja PhD⁸, Norbert Hubner MD^{5,6,9}, Paul J.R. Barton PhD^{1,2,4,10}, Stuart
7 A Cook PhD^{1,2,7,8}

8 ¹MRC-London Institute of Medical Sciences, Hammersmith Hospital Campus, London, UK.

9 ²Institute of Clinical Sciences, Faculty of Medicine, Imperial College, London, UK.

10 ³Wellcome Trust / NIHR 4i Clinical Research Fellow, Imperial College, London, UK.

11 ⁴National Heart and Lung Institute, Imperial College, London, UK.

12 ⁵Cardiovascular and Metabolic Sciences, Max Delbrück Center for Molecular Medicine in the
13 Helmholtz Association (MDC), Berlin, Germany.

14 ⁶DZHK (German Centre for Cardiovascular Research), Partner Site Berlin, Berlin, Germany.

15 ⁷National Heart Research Institute Singapore, National Heart Centre Singapore, Singapore.

16 ⁸Cardiovascular and Metabolic Disorders Program, Duke-National University of Singapore
17 Medical School, Singapore.

18 ⁹Charite, Universitätsmedizin Berlin, Berlin, Germany.

19 ¹⁰Royal Brompton and Harefield Hospitals, Guy’s and St. Thomas’ NHS Foundation Trust,
20 London UK

21 **Short title:**

22 Acute cardiac toxicities of interleukin 11

23 **Address for correspondence:**

24 Dr Mark Sweeney, London Institute of Medical Science, Imperial College London. W12 0NN.
25 msweeney@ic.ac.uk or Professor Stuart Cook, London Institute of Medical Science, Imperial
26 College London, W12 0NN. stuart.cook@imperial.ac.uk

27 **Total word count:** 8,610

28 **Manuscript main text word count:** 4,544

29 Abstract

30 Background

31 Interleukin 11 (IL11) was initially thought important for platelet production, which led to
32 recombinant IL11 being developed as a drug to treat thrombocytopenia. IL11 was later found
33 to be redundant for haematopoiesis and its use in patients is associated with unexplained cardiac
34 side effects. Here we identify previously unappreciated and direct cardiomyocyte toxicities
35 associated with IL11 therapy.

36 Methods

37 We injected recombinant mouse IL11 (rmIL11) into mice and studied its molecular effects in
38 the heart using immunoblotting, qRT-PCR, bulk RNA-seq, single nuclei RNA-seq (snRNA-
39 seq) and ATAC-seq. The physiological impact of IL11 was assessed by echocardiography *in*
40 *vivo* and using cardiomyocyte contractility assays *in vitro*. To determine the activity of IL11
41 specifically in cardiomyocytes we made two cardiomyocyte-specific *Il11ra1* knockout mouse
42 models using either AAV9-mediated and *Tnnt2*-restricted (vCMKO) or *Myh6* (m6CMKO) Cre
43 expression and an *Il11ra1* floxed mouse strain. In pharmacologic studies, we studied the effects
44 of JAK/STAT inhibition on rmIL11-induced cardiac toxicities.

45 Results

46 Injection of rmIL11 caused acute and dose-dependent impairment of left ventricular ejection
47 fraction (saline (2 μ L/kg), 60.4% \pm 3.1; rmIL11 (200 mcg/kg), 31.6% \pm 2.0; p <0.0001, n =5).
48 Following rmIL11 injection, myocardial STAT3 and JNK phosphorylation were increased and
49 bulk RNA-seq revealed upregulation of pro-inflammatory pathways (TNF α , NF κ B and
50 JAK/STAT) and perturbed calcium handling. SnRNA-seq showed rmIL11-induced expression
51 of stress factors (*Ankrd1*, *Ankrd23*, *Xirp2*), activator protein-1 (AP-1) transcription factor genes
52 and *Nppb* in the cardiomyocyte compartment. Following rmIL11 injection, ATAC-seq

53 identified epigenetic enrichment of the *Ankrd1* and *Nppb* genes and stress-responsive, AP-1
54 transcription factor binding sites. Cardiomyocyte-specific effects were examined in vCMKO
55 and m6CMKO mice, which were both protected from rmIL11-induced left ventricular
56 impairment and molecular pathobiologies. In mechanistic studies, inhibition of JAK/STAT
57 signalling with either ruxolitinib or tofacitinib prevented rmIL11-induced cardiac dysfunction.

58 Conclusions

59 Injection of IL11 directly activates JAK/STAT3 in cardiomyocytes to cause acute heart failure.
60 Our data overturn the earlier assumption that IL11 is cardioprotective and explain the serious
61 cardiac side effects associated with IL11 therapy, which questions its continued use in patients.

62 Clinical Perspective

63 What is new?

- 64 ● Injection of IL11 to mice causes acute and dose-dependent left ventricular impairment
- 65 ● IL11 activates JAK/STAT3 in cardiomyocytes to cause cell stress, inflammation and
66 impaired calcium handling
- 67 ● These data identify, for the first time, that IL11 is directly toxic in cardiomyocytes,
68 overturning the earlier literature that suggested the opposite

69 What are the clinical implications?

- 70 ● Recombinant human IL11 (rhIL11) is used as a drug to increase platelets in patients
71 with thrombocytopenia but this has severe and unexplained cardiac side effects
- 72 ● We show that IL11 injection causes cardiomyocyte dysfunction and heart failure, which
73 explains its cardiac toxicities that were previously thought non-specific
- 74 ● These findings have immediate translational implications as they question the
75 continued use of rhIL11 in patients around the world

76

77 Abbreviations

AAV9	Adeno-associated virus serotype 9
ANOVA	Analysis of variance
AP-1	Activator protein 1
ATACseq	Assay for transposase-accessible chromatin with sequencing
Bpm	Beats per minute
CM	Cardiomyocyte
ECG	Electrocardiogram
EGFP	Enhanced green fluorescent protein
ERK	Extracellular signal regulated kinase
FDR	False discovery rate
FOSL2	FOS like 2
GAPDH	Glyceraldehyde-3-phosphate dehydrogenase
GCS	Global circumferential strain
GSEA	Gene set enrichment analysis
HR	heart rate
IL6	Interleukin 6
IL11	Interleukin 11
IL11RA1	Interleukin 11 receptor A1
IP	Intraperitoneal
JAK	Janus kinase
JNK	c-Jun N-terminal kinase
KEGG	Kyoto encyclopaedia of genes and genomes
LV	Left ventricle
LVEF	Left ventricular ejection fraction
PBS	Phosphate buffered saline
PCR	Polymerase chain reaction
PSAX	Parasternal short axis
QPCR	Quantitative polymerase chain reaction
rhIL11	Recombinant human interleukin 11
RIPA	Radioimmunoprecipitation assay buffer
rmIL6	Recombinant mouse interleukin 6
rmIL11	Recombinant mouse interleukin 11
SEM	Standard error of the mean
STAT	Signal transducer and activator of transcription
TNFα	Tumour necrosis factor-alpha
UMAP	Uniform Manifold Approximation and Projection
vCMKO	Viral mediated cardiomyocyte <i>Il11ra1</i> knockout
VTI	Velocity time integral
WT	Wild type

78 Introduction

79 Interleukin 11 (IL11) is an elusive member of the interleukin 6 (IL6) family of cytokines, which
80 collectively signal via the gp130 co-receptor. Following its identification in 1990¹ recombinant
81 human IL11 (rhIL11) was found to increase megakaryocyte activity and peripheral platelet
82 counts in mice². Soon after, IL11 was developed as a therapeutic (Oprelvekin; Neumega) to
83 increase platelet counts in patients with chemotherapy-induced thrombocytopenia, received
84 FDA approval for this indication in 1998 and is still used to this day^{3,4}. In recent years, longer-
85 acting formulations of rhIL11 have been tested in pre-clinical studies and new clinical trials of
86 PEGylated rhIL11 in patients are anticipated⁵.

87 RhIL11 was also trialled to increase platelet counts in patients with von Willebrand factor
88 deficiency, myelodysplastic syndrome, cirrhosis and sepsis, and tested as a putative
89 cytoprotective agent in numerous other conditions, including myocardial infarction⁶ [**Table 1**
90 **and Suppl Table 1**]. However, it became apparent that IL11 is not required for basal or
91 compensatory blood cell or platelet counts in mice or humans: IL11 is in fact redundant for
92 haematopoiesis^{7,8}. Thus, the effects of injection of high dose rhIL11 on platelets appear non-
93 physiological and possibly reflect non-specific gp130 activity^{9,10}.

94 Unfortunately, injection of rhIL11 into patients has severe and hitherto unexplained cardiac
95 side effects. Up to 20% of patients given rhIL11 (50 mcg/kg) develop atrial arrhythmias, a high
96 proportion of individuals develop heart failure and rare cases of ventricular arrhythmias and
97 sudden death are reported^{11,12}. Furthermore, serum natriuretic peptide levels become acutely
98 and transiently elevated in patients receiving IL11 therapy, with B-natriuretic peptide levels
99 sometimes exceeding those diagnostic of heart failure.

100 While IL11 was previously thought to be cytoprotective, anti-inflammatory and anti-fibrotic in
101 the heart¹³⁻¹⁵ and other organs, recent studies by ourselves and others have challenged this
102 premise¹⁶⁻¹⁸. Indeed, experiments over the last five years have questioned the earlier literature
103 and IL11 is increasingly viewed as pro-inflammatory and pro-fibrotic. Given this large shift in
104 our understanding of IL11 and the fact that cardiomyocytes (CMs) robustly express IL11RA,
105 we devised experiments to determine whether IL11 is toxic to CMs and if this could explain
106 cardiac side effects associated with IL11 therapy in patients.

NCT Number	Title	Start Date	n	Status	Phase
Thrombocytopenia					
NCT03823079	Comparison of Interleukin-11 and rhTPO for Recurrent Colorectal Cancer Patients With Thrombocytopenia	Feb-19	50	Unknown status	2
NCT01663441	A Phase IIIa Study of Genetically Modified Recombinant Human Interleukin-11	Mar-15	62	Completed	3
NCT02314273	Effect of rhIL-11 in Patients With Thrombocytopenia for Childhood Acute Lymphocytic Leukaemia	Sep-11	120	Completed	4
NCT00886743	Study Evaluating The Effects Of Oprelvekin On Cardiac Repolarization In Subjects With Chemotherapy Induced Thrombocytopenia	Sep-09	19	Terminated	2
NCT00493181	Interleukin 11, Thrombocytopenia, Imatinib in Chronic Myelogenous Leukemia patients	Oct-05	8	Completed	2
Coagulopathy					
NCT00994929	Efficacy and Safety of IL-11 in DDAVP Unresponsive	Jan-10	9	Completed	2
NCT00524225	IL-11 in Adults With Von Willebrand Disease Undergoing Surgery	Feb-08	3	Terminated	2
NCT00524342	IL-11 in Women With Von Willebrand Disease and Refractory Menorrhagia	Jan-08	7	Completed	2
NCT00151125	Phase II Study of IL-11 (Neumega) in Von Willebrand Disease	Jul-04	12	Completed	2
Inflammatory Bowel Disease					
NCT00038922	Study Evaluating rhIL-11 in Left-Sided Ulcerative Colitis	Jun-02		Terminated	1
NCT00040521	Study Evaluating rhIL-11 in Active Crohn's Disease	Apr-02		Completed	2
Other					
NCT00012298	Radiolabeled Monoclonal Antibody Plus Rituximab With and Without Filgrastim and Interleukin-11 in Treating Patients With Relapsed or Refractory Non-Hodgkin's Lymphoma	Apr-01	81	Terminated	1/2
NCT03720340	Interleukin-11 Can Prevent and Treat of Radioactive Oral Mucitis	Oct-18	300	Unknown status	3

107 **Table 1. Human clinical trials registered with clinicaltrials.gov using recombinant human**
108 **interleukin 11.**

109 Methods

110 Detailed information on experimental methods of RNA and DNA analysis and cardiomyocyte
111 isolation protocols are provided in the supplementary material.

112 Animal studies

113 All mouse studies were conducted according to the Animals (Scientific Procedures) Act 1986
114 Amendment Regulations 2012 and approved by the Animal Welfare Ethical Review Body at
115 Imperial College London. Animal experiments were carried out under UK Home Office Project
116 License P108022D1 (September 2019). Wild type (WT) mice on a C57BL/6J background were
117 purchased from Charles River (Cat#632). They were bred in a dedicated breeding facility and
118 housed in a single room of the experimental animal facility with a 12-hour light-dark cycle and
119 provided food and water *ad libitum*. The *Il11ra1* floxed mouse (C57BL/6-Il11ra1^{em1Cook/J},
120 Jax:034465) has exons 4-7 of the *Il11ra1* gene flanked by loxP sites as has been described
121 previously¹⁹. In the presence of Cre-recombinase excision of exon 4-7 results in a non-
122 functional IL11 receptor.

123 Male myosin heavy chain 6 Cre (*Myh6-Cre*) mice (B6.FVB-Tg(*Myh6-cre*)2182Mds/J,
124 Jax:011038) were purchased from Jax (Bar Harbor, Maine, United States) as heterozygotes.
125 These mice were crossed with homozygous *Il11ra1* floxed females. In the second generation,
126 mice from generation one, heterozygous for the *Il11ra1* flox allele and heterozygous for the
127 Cre, were crossed with *Il11ra1* flox homozygotes to produce littermate experimental and
128 control animals.

129 Recombinant mouse interleukin-11 (rmIL11) (Z03052, Genscript, Oxford, UK) was dissolved
130 in phosphate-buffered saline (PBS) (14190144, ThermoFisher, MA, USA), and injected
131 intraperitoneally (IP) at a dose of 200 mcg/kg unless otherwise stated. Control mice received

132 an equivalent volume of saline (2 μ L/kg). Recombinant mouse interleukin-6 (Z02767,
133 Genscript) was dissolved in PBS and injected IP at a dose of 200 mcg/kg. Mice were randomly
134 assigned to a treatment group using a random number generator and syringes for injection were
135 prepared and blinded by a different investigator than administered the IP injection.

136 Genotyping

137 Genotype was confirmed with ear-notch DNA samples. DNA was extracted using a sodium
138 hydroxide digestion buffer, then neutralised with 1M Tris-HCl pH 8. *Il1ral* flox genotype
139 was confirmed with a single polymerase chain reaction (PCR) reaction yielding a PCR product
140 at 163bp for the wild type allele or 197bp in the transgenic allele. *Myh6*-Cre mice were
141 genotyped using two reactions for either the transgenic gene product of 295bp (or wild type
142 gene product of 300bp) along with an internal positive control (200bp). Primers used in these
143 reactions are detailed in supplementary table 2.

144 Viral Vector

145 The viral vector used in this study, AAV9-cTNT-EGFP-T2A-iCre-WPRE (VB5413), was
146 purchased from Vector Biolabs (Malvern, PA, USA). A codon optimised Cre was delivered
147 using an AAV9 capsid and under the control of the *Tnnt2* promoter. This was linked to an
148 enhanced green fluorescent protein (EGFP) reporter with a 2a self-cleaving linker. 1×10^{12}
149 genome copies or an equivalent volume of saline were injected into the tail veins of 8 - 9 week
150 old homozygous male *Il1ral* flox mice and from this point mice were housed separately from
151 saline-injected controls for 3 weeks prior to further experiments.

152 Echocardiography

153 Echocardiography was performed under light isoflurane anaesthesia using a Vevo3100
154 imaging system and MX550D linear transducer (Fujifilm Visualsonic Inc, ON, Canada).

155 Anaesthesia was induced with 4% isoflurane for 1 minute and maintained with 1-2%
156 isoflurane. Mice were allowed to equilibrate to the anaesthetic after induction for 9 minutes
157 before imaging was started. Heart rate measurement from single lead electrocardiogram (ECG)
158 recordings were taken at the completion of the equilibration period. Measurements of
159 ventricular ejection fraction (LVEF) was measured from m-mode images taken in the
160 parasternal short axis (PSAX) view at midventricular level and averaged across 3 heartbeats.
161 Global circumferential strain (GCS) measurements were also taken from the PSAX view and
162 analysed in a semi-automated fashion by the VevoStrain imaging software (VevoLab, version
163 5.5.0, Fujifilm Visualsonic). Aortic velocity time integral (VTI) was measured using pulse
164 wave doppler in the aortic arch and an average taken from 3 heart beats. The investigator was
165 blinded to the treatment group for all studies at both the imaging acquisition and analysis stages.

166 qPCR

167 The tissue was washed in ice-cold PBS and snap-frozen in liquid nitrogen. Total RNA was
168 extracted using TRIzol (15596026, Invitrogen, MA, USA,) in RNeasy columns (74106,
169 Qiagen, MD, USA). cDNA was synthesised using Superscript Vilo Mastermix (11755050,
170 Invitrogen). Gene expression analysis was performed using quantitative polymerase chain
171 reaction (qPCR) with TaqMan gene expression assay in duplicate over 40 cycles. *Ill1ral*:
172 custom TaqMan assay [**Suppl Table 3**], *Nppb*: Mm01255770_g1, *Rrad*: Mm00451053_m1.
173 Gene expression data were normalised to *Gapdh* expression (Mm99999915_g1) expression
174 and fold change compared to control samples was calculated using $2^{-\Delta\Delta Ct}$ method.

175 RNASeq

176 8 week old male C57BL/6J mice were injected with rmIL11 (200 mcg/kg) or an equivalent
177 volume of saline (2 μ L/kg). The left ventricle was excised and flash frozen 1, 3 or 6 hours after

178 injection. Libraries were sequenced on a NextSeq 2000 to generate a minimum of 20 million
179 paired end 60bp reads per sample.

180 Raw RNAseq data and gene-level counts have been uploaded onto the NCBI Gene Expression
181 Omnibus database and will be made available with accession number (GSE240804).

182 Single nuclei RNAseq

183 Single nuclei sequencing was performed on flash frozen LV tissue that was extracted from 8
184 week old male C57BL/6J mice 3 hours after injection with rmIL11 (200mcg/kg) or saline
185 (2 μ L/kg). The tissue was processed according to standard protocols as previously
186 described^{20,21}. Nuclei were purified by fluorescent activated cell sorting and libraries were
187 sequenced using HiSeq 4000 (Illumina, CA, USA) with a minimum depth of 20,000–30,000
188 read pairs per nucleus.

189 All single nuclei sequence data generated and analyzed in this study have been deposited as
190 BAM files at the NCBI Gene Expression Omnibus database and will be made available upon
191 request.

192 ATAC Seq

193 8 week old male C57BL/6J mice were given an IP injection with rmIL11 (200mcg/kg) or saline.
194 The heart was excised 3 hours after injection and flash-frozen tissue was sent to Active Motif
195 to perform assay for transposase-accessible chromatin with sequencing (ATAC-seq) analysis.

196 Protein Analysis

197 Protein extraction was performed on flash frozen tissue using ice-cold Pierce RIPA buffer
198 (89901, ThermoFisher) supplemented with protease inhibitors (11697498001, Roche, Basel,
199 Switzerland) and phosphatase inhibitors (4906845001, Roche). Tissue was lysed using a

200 Qiagen Tissue Lyser II with metallic beads for 3 mins at 30Hz. Protein quantification was
201 performed using a Pierce bicinchoninic acid assay colorimetric protein assay kit (23225,
202 ThermoFisher). 10-20 μ g of protein was loaded per well and run on a 4-12% bis-tris precast
203 sodium-dodecyl sulfate page gel (NP0323BOX, Invitrogen). Semi-dry transfer was performed
204 using the TransBlot Turbo transfer system (1704150, BioRad, CA, USA) and the membrane
205 was blocked in 5% bovine serum albumin (A3803, Sigma-Aldrich, MO, USA). Primary
206 antibodies raised against the following targets were used: signal transducer and activator of
207 transcription 3 (STAT3) (4904S, Cell signalling technology (CST), MA, USA), pSTAT3
208 Tyr705 (9145L, CST), Extracellular signal regulated kinase (ERK) (9101S, CST), pERK
209 (4695S, CST), total c-Jun-N-terminal kinase (JNK) (sc-7345, Santa-Cruz, TX, USA), phospho-
210 JNK (sc-6254, Santa-Cruz), green fluorescent protein (ab290, Abcam) Glyceraldehyde-3-
211 phosphate dehydrogenase (GAPDH) (2118L, CST). Appropriate secondary horseradish
212 peroxidase linked antibody was incubated for 1 hour with gentle agitation at room temperature
213 and developed using chemiluminescence blotting substrate (1705061, BioRad or 34095,
214 Thermofisher, depending on strength of signal).

215 Cardiomyocyte extraction

216 CMs were extracted from the heart of 12 week old male C57BL/6J mice. Mice were deeply
217 anaesthetized with ketamine and xylazine before the heart was harvested. Cells were incubated
218 in Tyrode solution (1mM Ca, 1mM Mg) or Tyrode solution supplemented with rmIL11 (10
219 ng/mL) for 2 hours before recording. Cells were paced at 1Hz (10V, 10ms pulse width). Cell
220 recordings were made using the Cytocypher high-throughput microscope (Cytocypher BV,
221 Netherlands) and the automated cell finding system was used to identify and take recordings
222 from 20 individual cells per heart per experimental condition. Calcium recordings were

223 performed by incubating CMs with Fura 2AM dye (1 μ M) for 20 mins before fluorescent
224 recordings were taken.

225 Statistics

226 Statistical analyses were performed in GraphPad Prism V9.5.0 unless otherwise stated.
227 Normality testing was performed using the Shapiro-Wilk test. Hypothesis testing for single
228 comparisons was done using an unpaired two ways Student's t-test for normally distributed
229 data or by Mann-Whitney U test for non-normally distributed data.

230 Comparisons involving male and female mice were performed using a two-way analysis of
231 variance (ANOVA) with Sidak's multiple comparisons testing. Changes in expression over
232 multiple time points were analysed using a one-way ANOVA with Sidak's multiple
233 comparisons testing. All graphs display the mean and standard error of the mean unless stated
234 otherwise. P-values in RNA seq analysis were corrected for multiple testing using the false
235 discovery rate (FDR) approach. A p-value and FDR of <0.05 was considered significant.

236 Hierarchical testing of nested data

237 Statistical analysis of the data from high throughput microscopy of extracted cardiomyocyte
238 experiments were analysed using a hierarchical statistical approach²². This approach tests for
239 clustering within the data as may occur due to differences in the quality of myocyte preparation
240 on different days. This uses a two-level random intercept model of linear regression. The
241 analysis was performed using R-studio and the data was presented as the mean and standard
242 deviation and effective n number taking the intraclass clustering into account.

243 Figures

244 Graphs were prepared in GraphPad Prism V9.5.0 and R studio (Version 2023.03.0).

245 Illustrations were created with Biorender.com and figures were arranged in Adobe Illustrator

246 (Version 23.0.4.).

247 Results

248 Injection of rmIL11 to mice causes acute left ventricular dysfunction

249 Injection of rmIL11 to male C57BL/6J mice resulted in a tachycardic response (544±13 beats
250 per minute (bpm), n=5) as compared to mice injected with saline (433±12 bpm, n=5) (Mann
251 Whitney test, p=0.0079) [Fig1A, B]. Mice injected with rmIL11 injection had impaired LVEF
252 (60.4%±3.1 vs 31.6±2.0, p<0.0001, n=5vs5), reduced GCS (-30.8%±2.3 vs -10.6±0.59,
253 p<0.0001, n=5vs5) and reduced VTI in the aortic arch (36.8mm±1.9 vs 20.2±2.2, p<0.0004,
254 n=5vs5) compared to mice injected with saline [Fig1C-F]. To serve as a related cytokine
255 control an equivalent dose (200 mcg/kg) of rmIL6 was injected which had no detectable acute
256 effects on cardiac function [Fig1A-F & Suppl Fig S1A, B].

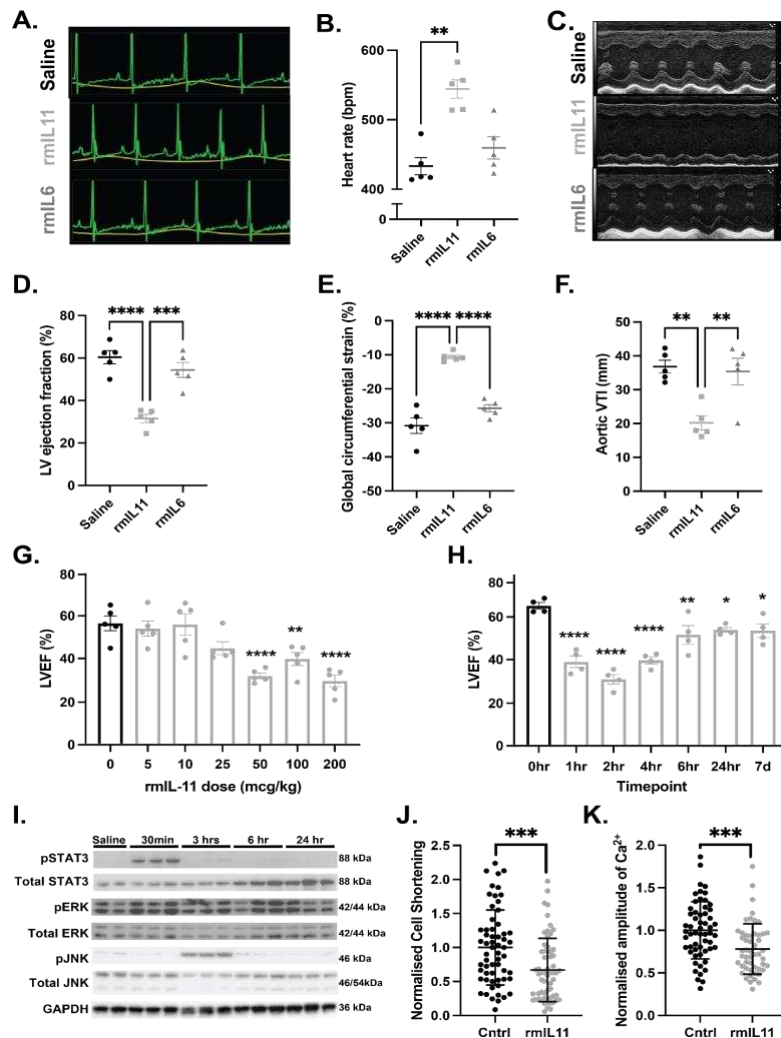
257 Dosing studies revealed that the effects of rmIL11 on heart rate and left ventricular (LV)
258 function were dose-dependent, consistent with physiological binding to and activation of the
259 IL11RA1 receptor. Cardiac impairment was evident at low doses and near-maximal effects
260 were seen with a dose of 50 mcg/kg, which is the dose typically given daily to patients with
261 thrombocytopenia post-chemotherapy [Fig1G]. The effect of rmIL11 was rapid with a nadir in
262 cardiac function at 2 hours post injection and recovery seen by 6 hours. However, recovery in
263 cardiac function was incomplete and mild LV impairment persisted for up to 7 days following
264 a single dose of rmIL11 [Fig1H].

265 IL11 causes impaired cardiomyocyte calcium handling

266 We next examined IL11 signalling pathways in cardiac extracts following rmIL11 injection,
267 which revealed early and short-lived phosphorylation of signal transducer and activator of
268 transcription 3 (p-STAT3) but no apparent ERK activation, which differs from acute signalling
269 effects in the liver and other organs²³ [Fig1I & Suppl Fig S1C]. Phosphorylation of JNK is a

270 stress related signalling pathway shown to be elevated in the mouse liver following IL11
271 treatment²³. In the myocardium JNK was phosphorylated at the 3 hour time point post rmIL11
272 injection by which stage STAT3 phosphorylation was declining [**Fig1I** & **Suppl Fig S1D**].

273 The effect of IL11 directly on CMs was analysed *in vitro* by treating isolated adult mouse CMs
274 with rmIL11 for 2 hours. CMs treated with rmIL11 demonstrated impaired contractility, as
275 compared to control cells (Control: 1.00 ± 0.177 ; rmIL11 (10 ng/mL): 0.669 ± 0.150 ,
276 $p < 0.000266$) [**Fig1J**]. Intracellular calcium transients revealed blunting of the peak calcium
277 concentration during systole in the presence of rmIL11 (Control: 1.00 ± 0.0972 ; rmIL11:
278 0.781 ± 0.0858 , $p < 0.00019$) [**Fig1K**].



279
280
281
282
283
284
285
286
287
288
289
290
291
292
293
294
295
296
297
298

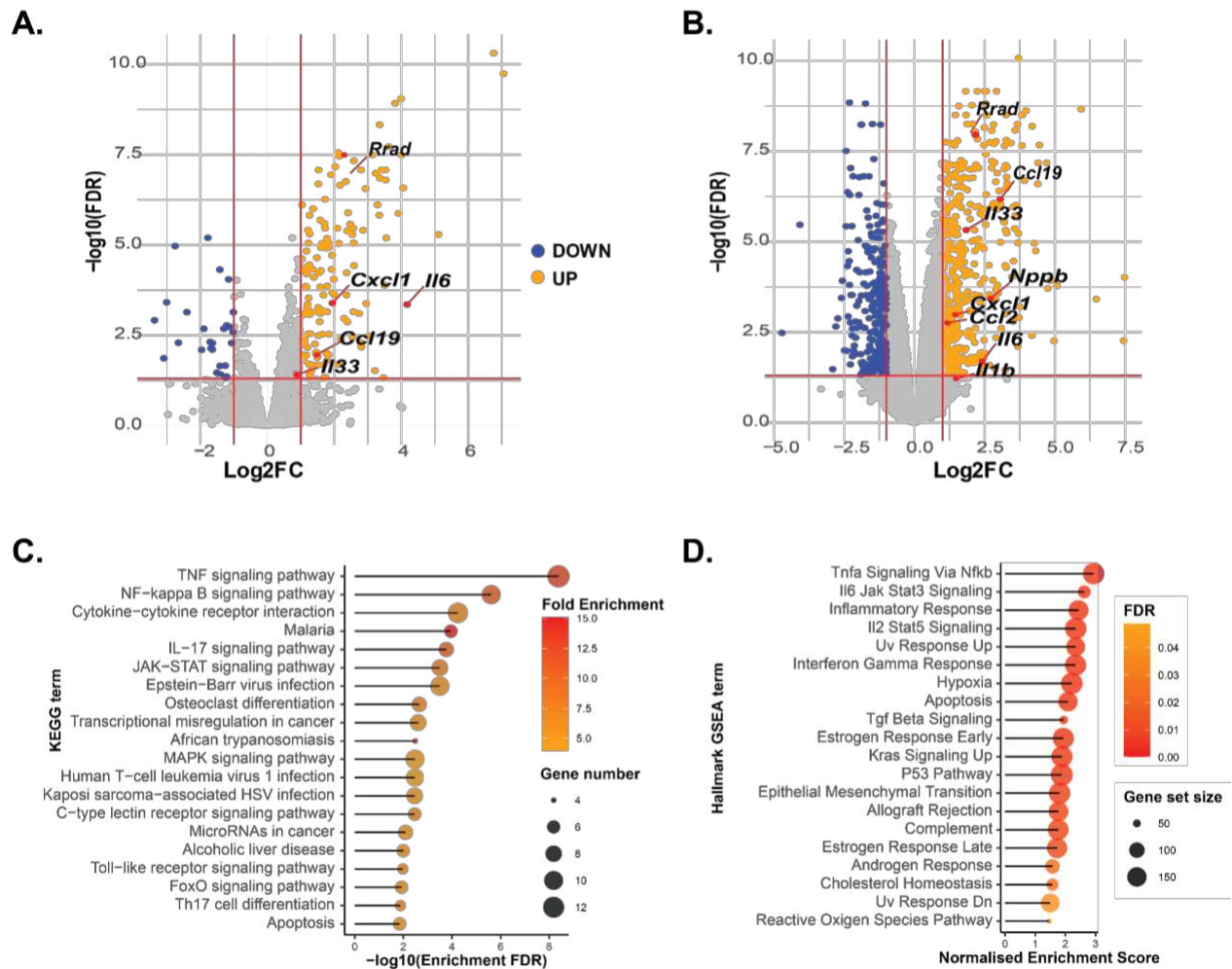
Figure 1. IL11 causes acute heart failure and impairs cardiomyocyte calcium handling. Male C57BL/6J mice were injected with rmIL11 (200 mcg/kg) (■), rmIL6 (200 mcg/kg) (▲) or an equivalent volume of saline (2 µl/kg) (●). (A) Representative electrocardiogram traces were recorded under light anaesthesia, 2 hours after intraperitoneal (IP) injection of saline, rmIL11 or rmIL6. (B) Quantification of heart rate (n=5 per group). (C) Representative m-mode images from echocardiography performed 2 hours after injection of saline, rmIL11 or rmIL6. (D) Quantification of left ventricular ejection fraction (LVEF), (E) global circumferential strain and (F) velocity time integral at the aortic arch (VTI) in each group (n=5 per group). (G) LVEF 2 hours after IP injection of rmIL11 to male mice at 0, 5, 10, 25, 50, 100 and 200 mcg/kg (n=5 per dose). (H) LVEF at baseline, 1, 2, 4, 6, and 24 hours, and 7 days after IP injection of rmIL11 (200 mcg/kg) (n=4 per timepoint). (I) Western blot of myocardial lysates from C57BL/6J male mice at baseline and 0.5, 3, 6 and 24 hours after IP rmIL11 injection (200 mcg/kg). Blots are probed for pSTAT3, total STAT3, pERK, total ERK, pJNK, total JNK and GAPDH. CMs isolated from male C57BL/6J mice were treated *in vitro* for 2 hours with media supplemented with rmIL11 (10 ng/mL) or non-supplemented media (Cntrl) (n=3 mice, 20 cells per mouse) and assessed for (J) contractility (effective n=9.7) and (K) the systolic change of intracellular calcium concentration (effective n=12). *Statistics: One-way ANOVA with Sidak's multiple comparisons test. CM data: two level hierarchical clustering. Significance denoted as *p<0.05, **p<0.01, ***p<0.001, ****p<0.0001.*

299 IL11 causes cardiac inflammation

300 The robust and early activation of STAT3 by IL11 led us to explore transcriptional changes
301 which might occur acutely within the myocardium in response to IL11 injection. Bulk RNA
302 sequencing was performed on LV tissue at 1, 3 and 6 hours following injection of rmIL11 and
303 compared to controls injected with saline.

304 Extensive and significant transcription changes were apparent at all timepoints (**1hr**, Up:145,
305 Down:27; **3hr**, Up:450, Down:303; **6hr**: Up: 268, Down:169; Log₂FC+/-1, FDR<0.05). Genes
306 differentially regulated included early upregulation of acute inflammatory genes (*Il6*, *Il1b* and
307 *Il33*), chemotactic factors such as (*Ccl2* and *Cxcl1*) and CM stress markers (*Nppb*, *Cnn2*,
308 *Ankrd1*) [**Fig2A, B**]. Kyoto Encyclopedia of Genes and Genomes (KEGG) analysis of the
309 differentially expressed genes at the 1-hour time point revealed the TNF α , NF- κ B and
310 JAK/STAT signalling were among the most significantly enriched terms [**Fig2C & Suppl Fig**
311 **S2A, C**]. A similar group of inflammatory terms were highlighted by Hallmark Gene Set
312 Enrichment Analysis including TNF α signalling via NF κ B, IL6 JAK/STAT and interferon-
313 gamma signalling [**Fig2D & Suppl Fig S2B, D**]. These transcriptional changes show that IL11
314 drives an acute proinflammatory response in the heart that is associated with an impaired
315 systolic function.

316 On closer inspection, the L-type calcium channel inhibitor *Rrad* was identified as one of the
317 most significantly upregulated genes at 1 hour (Fc:4.91, FDR:3.2e-8) and 3 hours (Fc:4.51,
318 FDR:9.2e-9) post rmIL11 treatment [**Fig2A, B**]. The *Rrad* protein product RAD-GTPase is a
319 well-characterised and potent inhibitor of calcium current through L-type calcium channels^{24,25}
320 and its acute upregulation may account for the changes in calcium transients seen in isolated
321 CM preparations.



322

323

324 **Figure 2. Transcriptional changes in the myocardium following rmIL11 injection.**

325 Volcano plot of all detected genes (A) 1 hour (n=3) and (B) 3 hours (n=4) after intraperitoneal

326 injection of rmIL11 at 200 mcg/kg. Red lines are drawn at Log₂Fc of 1 and -1 and FDR of

327 0.05. (C) Chart of most significantly enriched KEGG terms from at 1-hour post injection of

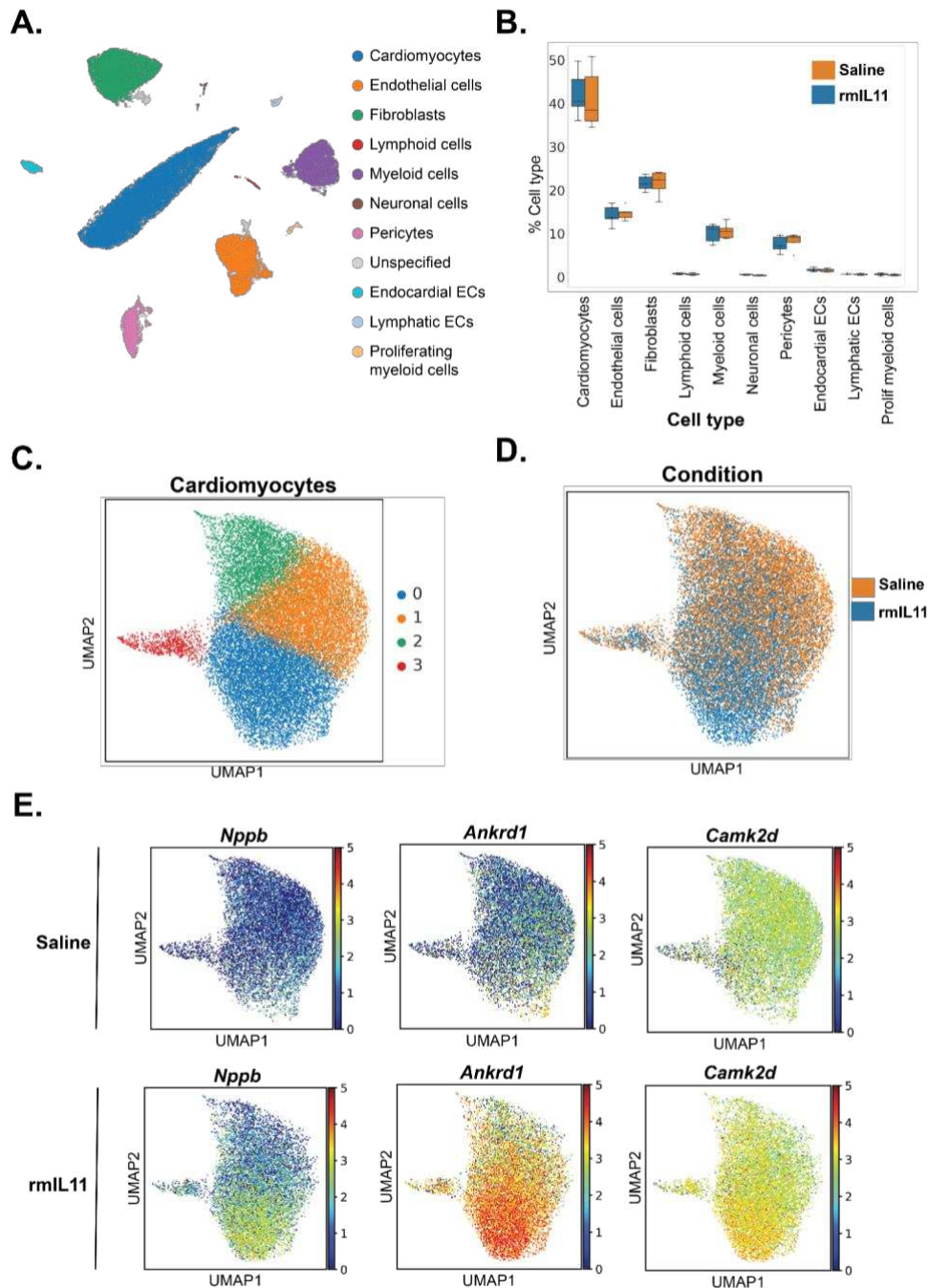
328 Hallmark gene sets from RNAseq data at 1 hour after injection of rmIL11 ranked by normalised

329 enrichment score.

330 Single nuclear sequencing reveals a cardiomyocyte stress signature

331 To examine cell-specific transcriptional responses and define any potential changes in cell
332 populations, we performed single nucleus RNA-sequencing (snRNAseq) experiments on hearts
333 3 hours post rmIL11 injection [**Fig 3A, Suppl Fig S3A-C, S4A & Suppl Table 4**]. This
334 revealed no significant change in cell populations overall, excluding immune cell infiltration
335 at this early time point [**Fig 3B**].

336 On closer analysis of CMs, this cell type segregated into four states with rmIL11-treated CM
337 mostly localised to state 0 [**Fig 3C, D**]. This state is defined by the expression of cardiomyocyte
338 stress factors including *Ankrd1*, *Ankrd23* and *Xirp2* [**Figure 3E & Suppl Fig S4B**]. *Ankrd1*
339 and *Ankrd23* are stress-inducible ankyrin repeat proteins which are elevated in dilated
340 cardiomyopathies^{26,27}. *Xirp2* encodes cardiomyopathy-associated protein 3 and is upregulated
341 in CMs in response to stress^{28,29}. Expression of *Nppb*, a canonical heart failure gene, was
342 similarly elevated [**Fig 3E**]. Overall, the most enriched pathway from KEGG analysis of CM-
343 specific differentially expressed genes, irrespective of state, was “Ribosome” with 93 out of
344 130 genes significantly upregulated (Fold enrichment:4.5, FDR:2.3e-46), perhaps related to the
345 large effects of IL11 on protein translation and/or a pro-hypertrophic response of stressed CMs
346 [**Suppl Fig S5**]³⁰.



347
348
349
350
351
352
353
354
355
356

Figure 3. Single nuclear RNA sequencing reveals an IL11-induced cardiomyocyte stress signature. (A) UMAP embedding of all cell types from the left ventricle of male C57BL/6J mice 3 hours after intraperitoneal injection of rmIL11 (200 mcg/kg) or an equivalent volume of saline (n=5). (B) Comparison of cellular composition of the left ventricle in rmIL11 treated mice compared to saline treated mice. (C) UMAP embedding of cardiomyocyte fraction. 4 distinct clusters are identified based on gene expression. (D) UMAP embedding of cardiomyocytes annotated with the treatment group. (E) UMAP embedding of cardiomyocyte fraction of saline or rmIL11 treated cardiomyocytes annotated with relative expression of *Nppb*, *Ankrd1*, and *Camk2d*.

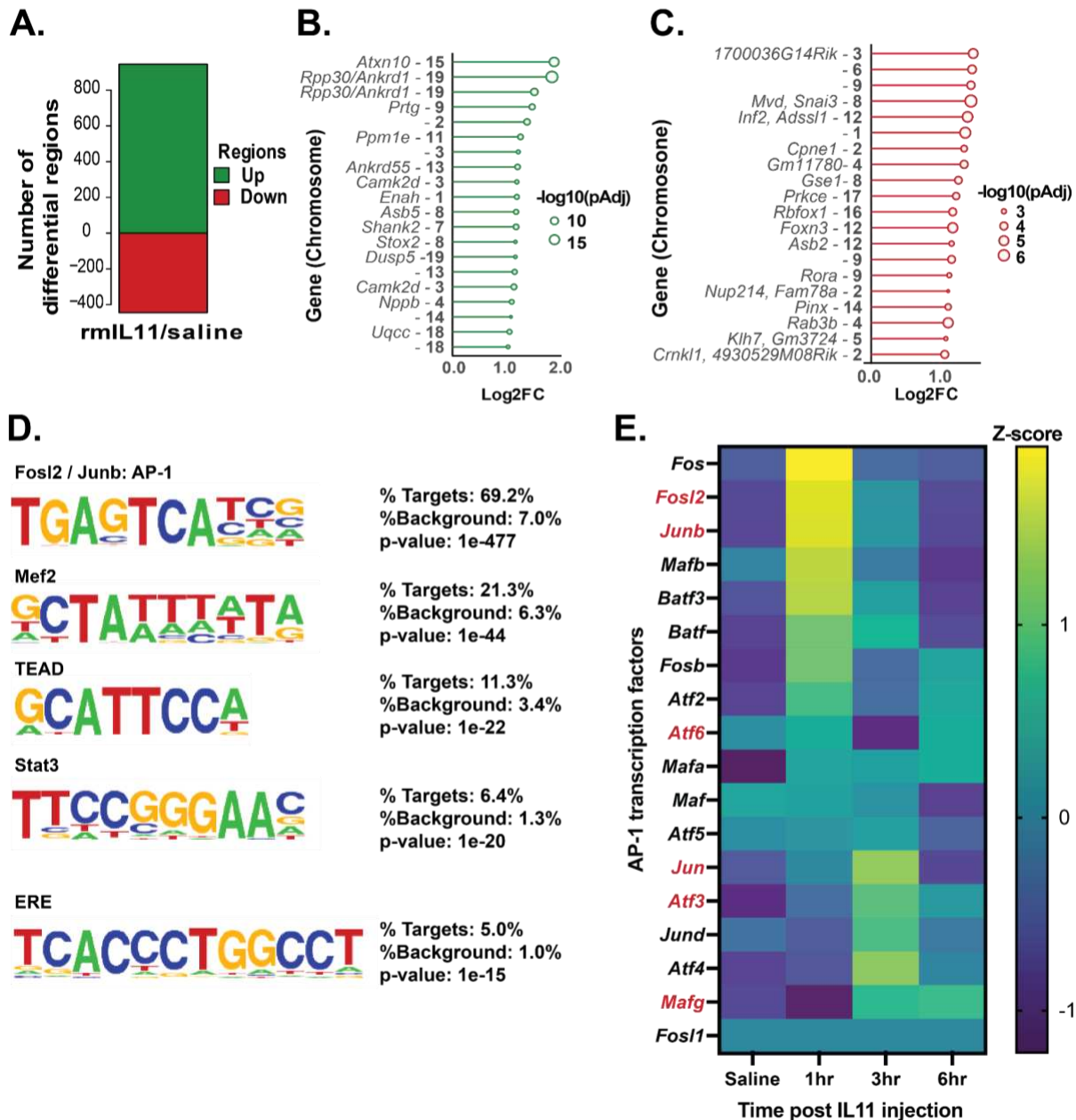
357 ATAC-Seq highlights AP-1 family genes

358 To better understand the molecular changes induced by IL11 in the heart, we performed Assay
359 for Transposase-Accessible Chromatin using sequencing (ATAC-seq) analysis. This
360 methodology identifies regions of the genome undergoing epigenetic variation to make
361 transcription factors binding sites more or less accessible.

362 Following IL11 administration, there were a large number of loci with variation in DNA
363 accessibility (increased, 945; reduced, 445; shrunkenLog2FC:±0.3, Padj<0.1) [**Fig 4A &**
364 **Suppl Table 5**]. The top twenty most differentially enriched regions [**Fig 4B, C**] include areas
365 adjacent to *Camk2d*, *Ankrd1* and *Nppb*, stress and calcium handling genes that we had already
366 found to be upregulated in CMs by snRNAseq [**Fig 3E, Fig 4B & Suppl Table 4**].

367 DNA motif analysis of sequences captured by ATAC-seq, revealed the most enriched motifs
368 after rmIL11 treatment were targets for FOSL2 and JUNB transcription factors [**Fig 4D &**
369 **Suppl Table 6**]. These genes belong to the activator protein-1 (AP-1) transcription factor
370 family, which is important for cardiomyocyte stress responses, cardiac inflammation and
371 fibrosis.^{31,32} Notably, the STAT3 binding motif was also highly enriched.

372 We revisited our bulk RNA-seq data to examine the expression of the AP-1 transcription factor
373 family transcripts after rmIL11 injection. This revealed that almost all of the AP-1 family
374 transcripts are upregulated in the heart after rmIL11 [**Fig 4E**]. We then queried the snRNA-seq
375 data and observed that *Fosl2*, *Junb*, *Atf6*, *Jun*, *Atf3* and *Mafg* are all significantly differentially
376 expressed in cardiomyocytes following rmIL11 injection [**Fig 4E and Suppl Table 4**].



377
378
379
380
381
382
383
384
385
386
387

Figure 4. ATAC-Seq reveals a stress signature that occurs acutely in the myocardium after rmIL11 injection. (A) Number of positively and negatively enriched genomic regions identified by ATAC-Seq analysis of the myocardium 3 hours after injection of rmIL11 (n=4). (B) Top 20 most strongly enriched DNA regions in ATAC-seq analysis and adjacent genes, when present. (C) Top 20 most strongly negatively enriched DNA regions in ATAC-seq analysis and adjacent genes. (D) De novo Homer motif analysis of ATAC-seq data most highly enriched motifs in myocardial samples. (E) Heatmap of AP-1 transcription factor family members from bulk RNA sequencing data of myocardium at baseline, 1, 3 and 6 hours after rmIL11 injection. Genes differentially expressed in cardiomyocytes in single nuclear RNA sequencing data are highlighted in red.

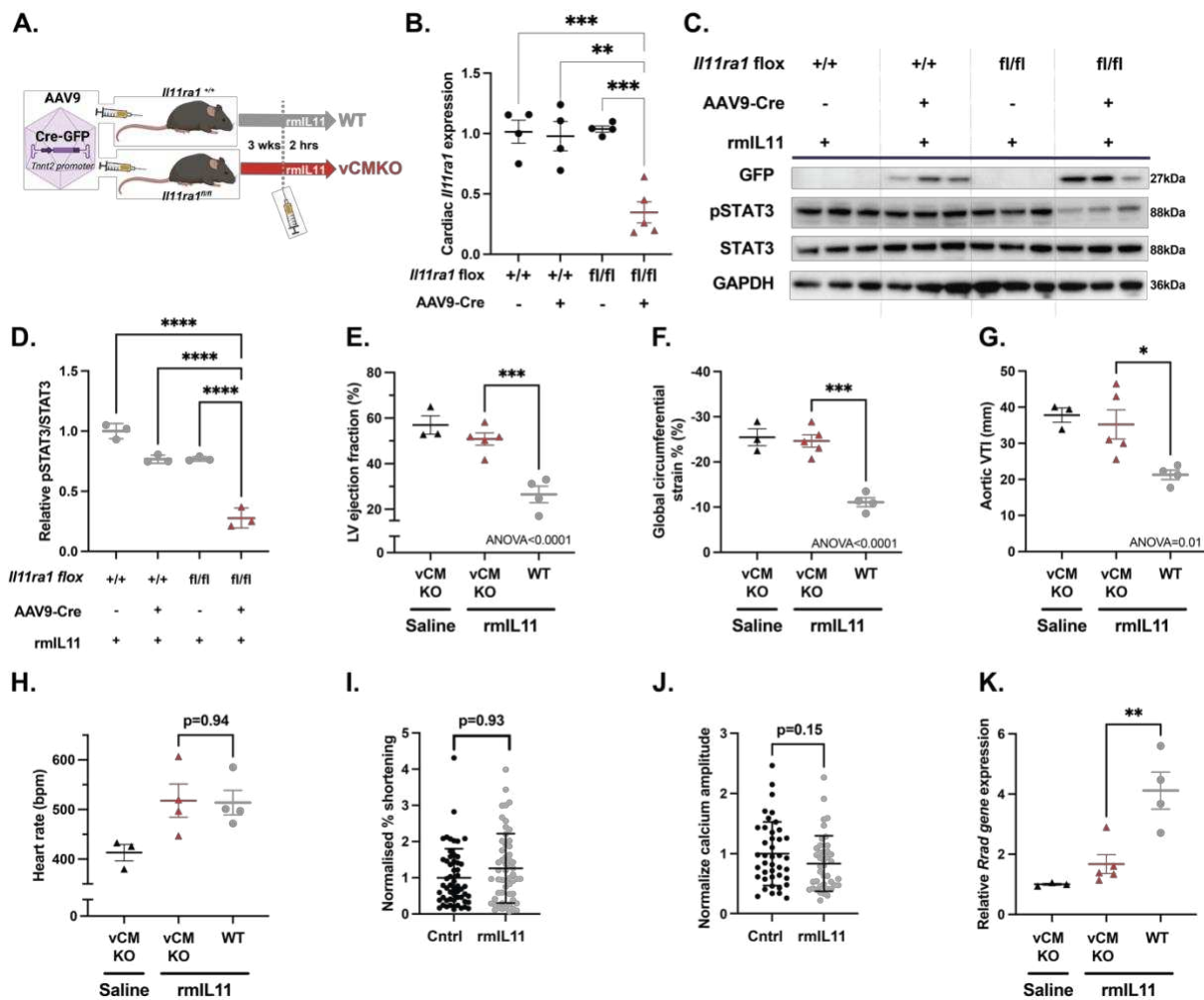
388 Viral-mediated CM-specific deletion of *Il1ral*

389 To test whether the acutely negative inotropic effects of IL11 and the signature of increased
390 CM stress are specifically mediated via IL11 activity in CMs, we proceeded to conditionally
391 delete *Il1ral* in CMs in the adult mouse. We used an adeno-associated virus serotype 9
392 (AAV9) vector to express *Tnnt2*-dependent *Cre*-recombinase in CMs of *Il1ral* floxed mice,
393 which effectively removed the floxed exons to generate mice with viral-mediated deletion of
394 *Il1ral* in CMs (vCMKO mice) [Fig 5A, B]. Effective transfection in the myocardium was
395 confirmed by immunoblotting for GFP which is co-expressed with the *Cre*-recombinase [Fig
396 5C]. Notably, vCMKO mice had diminished myocardial p-STAT3 following injection of
397 rmIL11, which demonstrates that IL11 activates JAK/STAT3 in CMs [Fig 5C, D].

398 As compared to mice injected with saline, WT mice injected with rmIL11 had impaired LVEF
399 (WT+rmIL11: 26.5%±3.6), whereas vCMKO injected with rmIL11 had a mean LVEF
400 (vCMKO+rmIL11: 50.8%±2.7) that was indistinguishable from saline-injected controls
401 (vCMKO+saline: 57.0%±4.0) (n=3-5 per group) [Fig 5E]. Similar changes were seen in GCS
402 (vCMKO+saline: -25.5%±1.9, vCMKO+rmIL11:-24.6%±1.4, WT+rmIL11: -11.1%±1.0,
403 p<0.0001) and VTI in the aortic arch (vCMKO+saline: 37.8cm±1.9, vCMKO+rmIL11:
404 35.2cm±4.03, WT+rmIL11: 21.3cm±1.31, p<0.0371) [Fig 5F, G]. Interestingly, this
405 experimental model still developed tachycardia following IL11 treatment, as seen in WT mice
406 [Fig 5H].

407 We performed experiments in CMs isolated from adult mice. Unlike CMs isolated from WT
408 animals [Fig 1J, K], CM from vCMKO mice did not have a reduction in cell shortening in
409 response to stimulation with rmIL11, as compared to unstimulated cells (Cntrl: 1.0±0.11,
410 vCMKO: 1.26±0.13, p=0.93, n=53.6). Similarly, peak calcium concentration was not blunted
411 by rmIL11 in vCMKO CMs (Cntrl: 1.0±0.088, vCMKO: 0.83±0.076. p=0.15, n=36.3) [Fig 5I,

412 **J]**. As such, IL11 effects in CMs are dependent on *Il1ral* expression in CMs. Consistent with
413 these changes in calcium signalling at a cellular level, qPCR of myocardial tissue of vCMKO
414 mice prevented elevation of *Rrad* compared to control mice following rmIL11 injection [**Fig**
415 **5K]**.



416
417
418
419
420
421
422
423
424
425
426
427
428
429
430
431
432
433
434
435

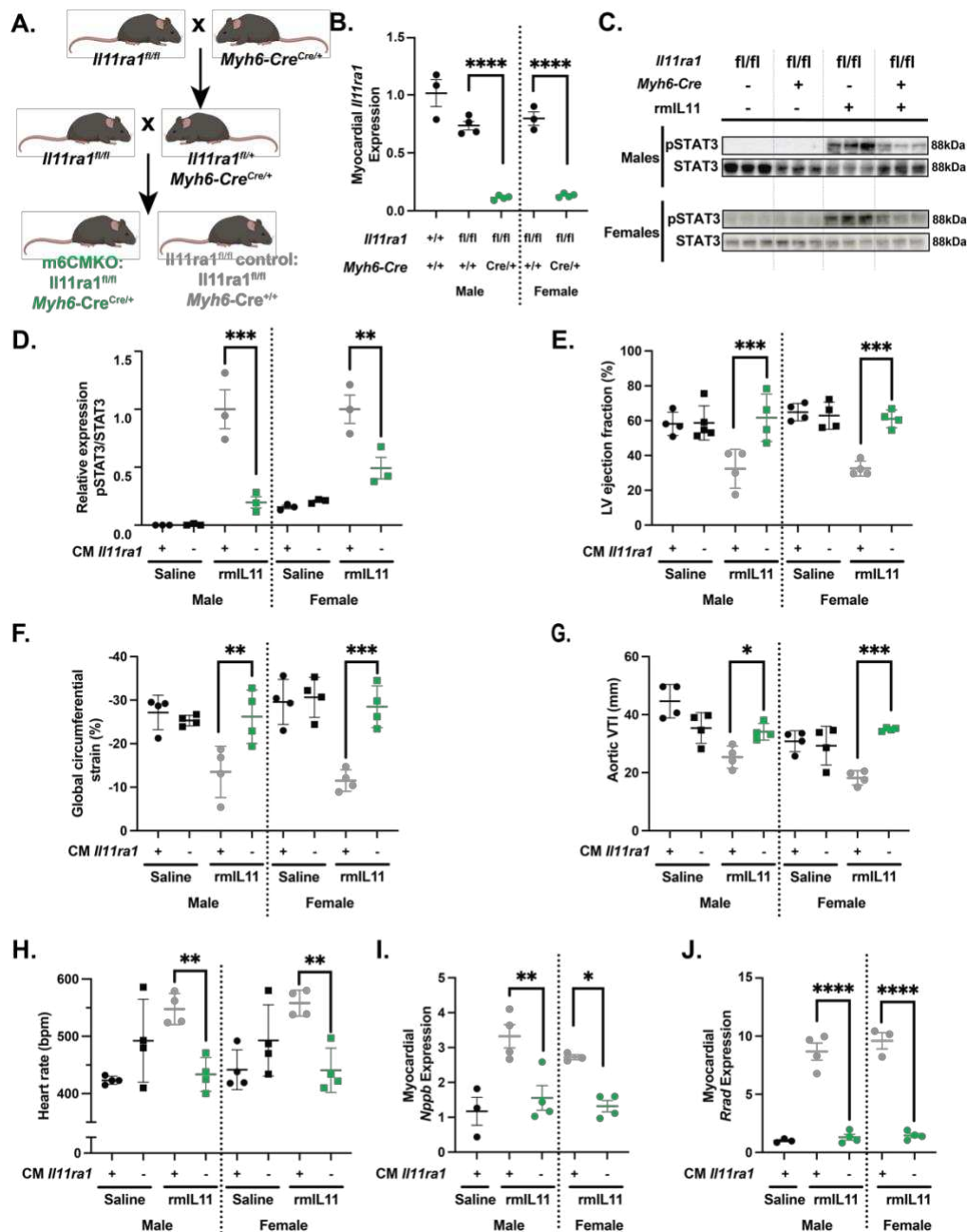
Figure 5. Viral-mediated *Il11ra1* deletion in adult cardiomyocytes protects against IL11-driven cardiac dysfunction. (A) Schematic of experimental design for AAV9 mediated delivery of *Tnnt2* promoter driven Cre-recombinase to male *Il11ra1^{fl/fl}* or *Il11ra1^{+/+}* mice. (B) QPCR of relative myocardial expression of *Il11ra1* in *Il11ra1^{+/+}* or *Il11ra1^{fl/fl}* injected with AAV9-Cre or vehicle. (C) Western blot from myocardial lysate following rmlIL11 injection (200 mcg/kg) in *Il11ra1^{+/+}* or *Il11ra1^{fl/fl}* treated with either AAV9-Cre or saline (n=3). The membrane was probed with primary antibodies against GFP, pSTAT3, STAT3, and GAPDH. (D) Quantification of relative pSTAT3/STAT3 from (C). Echocardiographic assessment of vCMKO mice injected with rmlIL11 (200 mcg/kg) (▲) or saline (▲) were compared to WT mice injected with rmlIL11 (200 mcg/kg) (●). (E) Left ventricular ejection fraction, (F) global circumferential strain and (G) velocity time integral at the aortic arch and (H) heart rate were measured 2 hours after treatment (n=4). (I) Contractility (effective n = 53.6) and (J) peak calcium amplitude (effective n = 36.3) in CMs isolated from vCMKO mice and treated for 2 hours *in vitro* with rmlIL11 containing media (10 ng/mL) or normal media (n=3 mice, 20 cells per mouse). (K) QPCR of myocardial expression of *Rrad* 2 hours vCMKO mice injected with rmlIL11 (200 mcg/kg) (▲) or saline (▲) compared to WT mice injected with rmlIL11 (200 mcg/kg) (●) *Graphs CM data: mean ± standard deviation. Statistics: One-way ANOVA with Sidak's multiple comparisons testing. CM data: two level hierarchical clustering. Significance denoted as *p<0.05, **p<0.01, ***p<0.001, ****p<0.0001.*

436 Germline deletion of *Il1ral* in cardiomyocytes

437 We then used a complementary, germline deletion methodology to validate the CM-specific
438 effects of IL11 seen in vCMKO mice by crossing *Il1ral* flox mice with *Myh6-Cre*
439 (m6CMKO) mice³³ [Fig 6A]. This approach achieved a more pronounced and consistent
440 knockdown of *Il1ral* that enabled experiments to be scaled across sexes [Fig 6B]. As seen in
441 the vCMKO strain, m6CMKO mice of both sexes had reduced p-STAT3 following rmIL11
442 injection, which further established effective *Il1ral* locus recombination in this strain and
443 reaffirms IL11-specific signalling in CMs [Fig 6C, D].

444 Having established the m6CMKO strain, we examined the effects of rmIL11 on cardiac
445 function in these mice [Suppl Table 7]. When injected with rmIL11, *Il1ral*^{fl/fl} control mice
446 had significantly reduced LVEFs whereas the LVEF of m6CMKO was similar to that of
447 m6CMKO mice injected with saline [Fig 6E]. Similarly, following rmIL11 injection, GCS and
448 VTI in the aortic arch were impaired in control mice expressing *Il1ral* but not in m6CMKO
449 mice [Fig 6F, G]. It was evident that the molecular and cardiovascular phenotypes of
450 m6CMKO mice injected with rmIL11 largely replicated those observed in the vCMKO mice.
451 However, different to the vCMKO strain, the m6CMKO mice were protected against IL11-
452 induced tachycardia. [Fig 6H].

453 In molecular studies of myocardial extracts, *Nppb* was upregulated in *Il1ral*^{fl/fl} control mice in
454 response to rmIL11 injection, but this was not seen in m6CMKO mice [Fig 6I]. Similarly,
455 following rmIL11 injection the L-type calcium channel inhibitor *Rrad* was upregulated in
456 *Il1ral*^{fl/fl} controls but not in m6CMKO mice [Fig 6J].



457
 458 **Figure 6. Germline deletion of $Il11ra1$ in cardiomyocytes prevents IL11-induced cardiac**
 459 **toxicities.** (A) Breeding strategy to generate m6CMKO mice and litter-mate $Il11ra1^{fl/fl}$
 460 controls. (B) QPCR of $Il11ra1$ gene expression in $Il11ra1^{fl/fl}$ controls and m6CMKO mice
 461 compared to male wild type C57BL/6J controls. (n=4) (C) Westerns blot of phospho-STAT3
 462 and total STAT3 signalling in male and female $Il11ra1^{fl/fl}$ controls and m6CMKO mice with
 463 and without rmlL11 treatment. (D) Quantification of relative pSTAT and STAT3 expression.
 464 Male and female m6CMKO mice (CM $Il11ra1$ -) were treated with saline (■) or rmlL11 (■) and
 465 compared to wild type mice (CM $Il11ra1$ +) treated with saline (●) or rmlL11 (●) (n=4). (E)
 466 left ventricular ejection fraction, (F) global circumferential strain, (G) velocity time integral
 467 (VTI) in the aortic arch and (H) heart rate was measured 2 hours after rmlL11 injection. (n=4).
 468 QPCR analysis of relative expression of (I) $Nppb$ and (J) $Rrad$ in the myocardium following
 469 rmlL11 treatment of m6CMKO mice and $Il11ra1^{fl/fl}$ control mice (n=4). *Statistics: Comparison*
 470 *between groups by two-way ANOVA with Sidak's multiple comparisons. p-values denoted as*
 471 **<0.05, **<0.01, ***<0.001, ****<0.0001).*

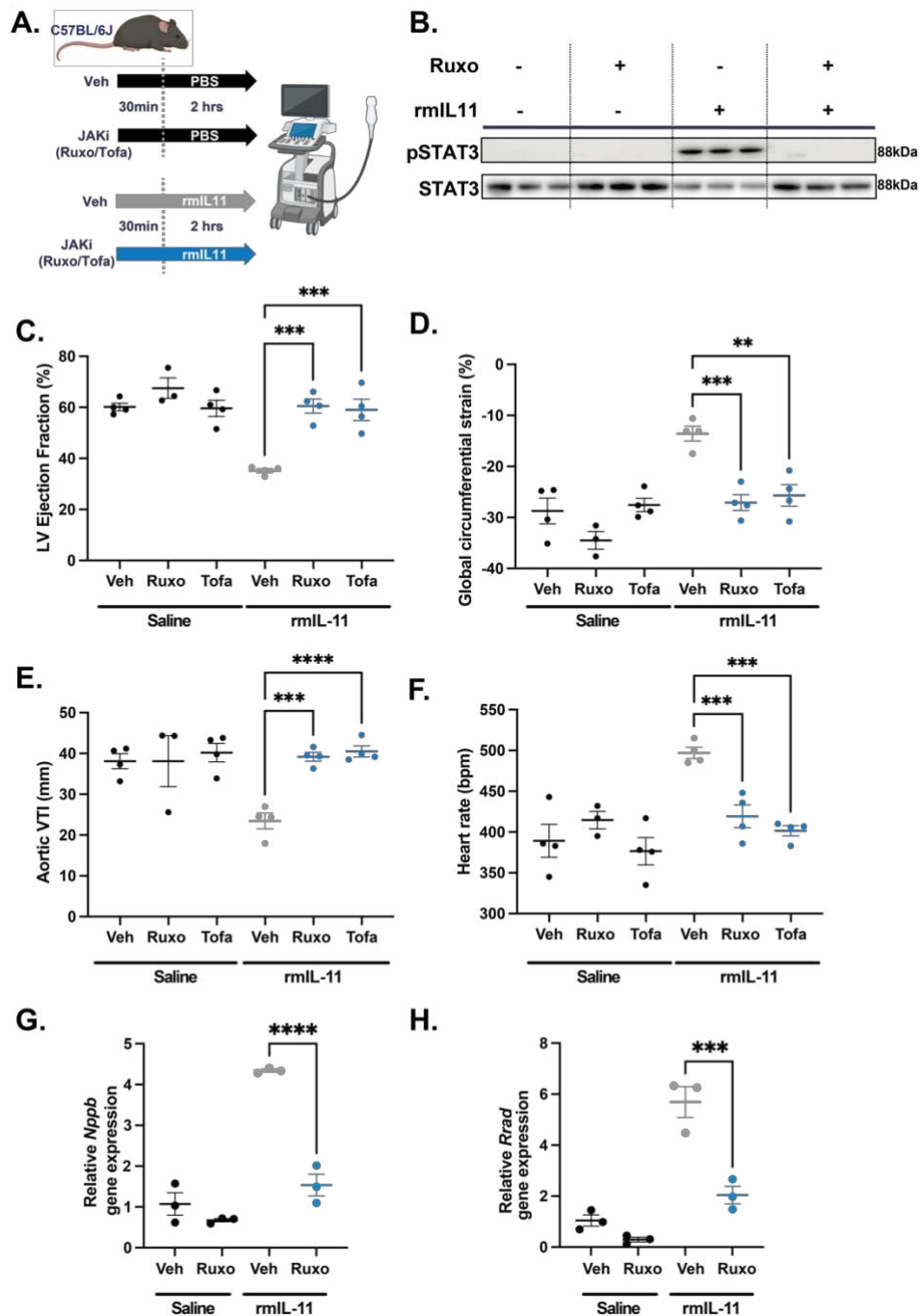
472 JAK inhibition protects against IL11-induced cardiac dysfunction

473 Canonical IL11 signalling through the IL11RA/gp130/JAK/STAT3 pathway has recently been
474 implicated in the acute pro-inflammatory effects of IL11³⁴ and activation of STAT3 in the heart
475 was immediate and pronounced following IL11 injection [**Fig 1I**]. To determine the functional
476 relevance of JAK/STAT3 activation in the heart we pretreated mice with ruxolitinib (30
477 mg/kg), which inhibits JAK1/2 activation, prior to injection of rmIL11 [**Fig 7A**].

478 We confirmed that administration of ruxolitinib at 30 mg/kg prevented activation of
479 JAK/STAT3 signalling by immunoblotting [**Fig 7B**]. Having established the efficacy of
480 ruxolitinib we studied its effect on cardiac physiology in 8 week old wild type male mice
481 injected with rmIL11. Ruxolitinib alone had no effect on LV function [**Fig 7C**]. Following
482 injection of rmIL11, and as compared to buffer injected controls, mice pretreated with
483 ruxolitinib had better LVEF (60.5%±2.79 vs 35.2%±0.79; p=0.0005), GCS (-27.1%±1.56 vs -
484 13.6%±1.44 vs, p=0.0009) and aortic VTI (39.2cm±10.9 vs 23.4cm±1.92, p=0.0001) [**Fig 7C-**
485 **E**]. Ruxolitinib pretreatment also prevented rmIL11-induced tachycardia (497±6.8 vs
486 419±14.1, p=0.0008) [**Fig 7F**]. As seen with m6CMKO, JAK inhibition prevented stress
487 associated transcriptional changes in the heart of *Nppb* and *Rrad* [**Fig 7G, H**].

488 To exclude off-target effects and to replicate findings, the study was repeated with a second
489 JAK inhibitor (tofacitinib, 20 mg/kg). As seen with ruxolitinib, pretreatment with tofacitinib
490 protected against the varied deleterious effects of IL11 on cardiac function compared to vehicle
491 treated controls: LVEF (59.0±4.16, p=0.0007), GCS (-25.7±2.10, p=0.002), VTI in the aortic
492 arch (40.5±1.36, p<0.0001), and tachycardia (401±6.23, p=0.0002). [**Fig 7C-E**].

493



494
495
496
497
498
499
500
501
502
503
504
505
506
507

Figure 7. The acute toxic effects of rmIL11 are mediated via JAK/STAT signalling. (A) Schematic of the pretreatment of wild type male C57BL/6J mice with JAK inhibitor (JAKi) or vehicle (Veh) 30 mins before administration of recombinant mouse IL11 (rmIL11) or saline. (B) Western blot of myocardium lysate in mice treated with a combination of ruxolitinib (30 mg/kg) or vehicle and saline or rmIL11. Membranes have been probed for pSTAT3 and STAT3 (n=3). Mice treated with a combination of vehicle (Veh), ruxolitinib (Ruxo) or tofacitinib (Tofa) and either saline or rmIL11 had an echocardiogram performed 2 hours after treatment which measured (C) left ventricular ejection fraction, (D) global circumferential strain, (E) velocity time integral (VTI) in the aortic arch and (F) heart rate (n=4). QPCR of myocardial tissue from combinations of Ruxo and rmIL11 treatments of (G) *Nppb* expression and (H) *Rrad* expression (n=3). Statistics: Comparison between groups by one-way ANOVA with Sidak's multiple comparisons test. Significance denoted as denoted * $p < 0.05$, ** $p < 0.01$, **** $p < 0.0001$.

508 Discussion

509 In some healthcare systems, rhIL11 is used routinely to increase platelet counts in patients with
510 thrombocytopenia but this can cause serious cardiac complications that are unexplained and
511 thought non-specific. RhIL11 has also been trialled in a different context, as a cytoprotective
512 agent, in patients across a range of other medical conditions (e.g. colitis, myocardial infarction,
513 arthritis, cirrhosis), [Table 1 & Supl Table 1] as IL11 was previously thought to be anti-
514 inflammatory and anti-fibrotic¹⁶. As such, many thousands of patients have received, and
515 continue to receive, rhIL11 in clinical trials and as part of routine medical care. Long-acting
516 formulations of rhIL11 have recently been devised and new clinical trials of rhIL11 are
517 proposed⁵.

518 The cardiac side effects of rhIL11, while unexplained, have long been recognised and a small
519 clinical trial was initiated in 2009 to determine if rhIL11 (50 mcg/kg) had an effect on cardiac
520 conduction (NCT00886743). This trial was terminated prematurely at the request of the
521 sponsor and no formal conclusions were made. Other studies looking at the effects of injection
522 of human IL11 to adult rats showed no effects on cardiac phenotypes and studies of human
523 atrial myocytes were similarly negative^{35,36}. We suggest that, for these reasons, the severe
524 cardiac side effects of rhIL11 therapy have been explained away as indirect, non-specific and
525 thus sidelined³⁶.

526 We found that injection of species-matched rmIL11 to mice caused acute and dose-dependent
527 LV impairment that was mediated via IL11's action in IL11RA1 expressing CMs. CMs
528 exposed to IL11 displayed perturbed calcium handling, upregulated cellular stress factors
529 (*Ankrd1*, *Ankrd23*, *Xirp2*, *Nppb*) and had exhibited increased inflammation (TNF α , NF κ B and
530 JAK/STAT). These findings further redress the earlier literature on IL11 activity in the heart
531 where it was believed to be anti-fibrotic¹⁴, which appears inaccurate³⁰, and that it was

532 cytoprotective in CMs^{13–15}, which we challenge here. In retrospect, the use of rhIL11 in a
533 clinical trial of patients with myocardial infarction was likely ill-founded⁶.

534 The powerful enrichment of the AP-1 family of transcription factors following rmIL11
535 injection, seen in bulk RNA-seq, snRNA-seq and ATAC-seq was unexpected and likely has
536 detrimental effects in the mouse heart^{31,37}. AP-1 family activation is not immediately
537 downstream of IL11:IL11RA:gp130 signalling and thus, the early IL11-stimulated activation
538 of JAK/STAT3 likely primes CMs to upregulate, activate and respond to AP-1 transcription
539 factors. In the injured zebrafish heart, AP-1 contributes to sarcomere disassembly and
540 regeneration³⁸, which is IL11-dependent³⁹, providing an evolutionary context for IL11-
541 mediated effects in the heart⁴⁰.

542 Our use of two mouse models of CM-specific *Il1ral* deletion show and replicate that the
543 effects of rmIL11 on cardiac function are via direct cardiotoxic effects on CMs and are not
544 explained by changes in circulating volume, as has previously been suggested³⁶. The models
545 used in this study involved the administration of a single dose of rmIL11 however in clinical
546 practice, courses of therapy can involve daily infusions of rhIL11 for up to 21 days between
547 chemotherapy cycles which are likely to compound the effect on the heart, specifically on
548 fibrotic pathologies that are slow to establish³⁰.

549 There are several limitations to our study. The discrepancy between the tachycardia seen in
550 vCMKO but not m6CMKO mice suggests a direct effect of IL11 on sinoatrial node, which is
551 differentially deleted for *Il1ral* between the models, was not explored. We did not determine
552 the putative roles of *Rrad* or *Camk2d* in IL11-induced contractile dysfunction, which should
553 be investigated more fully in follow-on studies. Effects on human CMs were not examined,
554 although we have observed conserved effects of IL11 on multiple cellular phenotypes in varied
555 human and mouse cell types (e.g. fibroblasts, hepatocytes, epithelial cells)^{16,23}. Whether

556 endogenous IL11 is toxic to CMs and negatively inotropic in heart failure syndromes is not
557 known and we cannot extrapolate from the data seen with acute, high dose injection of
558 recombinant protein. The cardiac side effects associated with IL11 include arrhythmias
559 (notably atrial fibrillation and flutter) that we did not study here.

560 In conclusion, we show for the first time that IL11 injection causes IL11RA-dependent, CM-
561 specific toxicities and acute heart failure. These data may explain the serious cardiac side
562 effects that occur with rhIL11 therapy, which have been overlooked. Our findings question the
563 ongoing use of rhIL11, and its further development⁵, in patients with thrombocytopenia while
564 identifying novel toxic effects of IL11 in the cardiomyocyte compartment of the heart.

565 Grant Funding:

566 This work was supported by grant funding from Wellcome Trust (203928/Z/16/Z), Foundation
567 Leducq [16 CVD 03], the Medical Research Council (UK), The NIHR Biomedical Research
568 Centre Imperial College London, the National Medical Research Council (NMRC) Singapore
569 STaR award (NMRC/STaR/0011/2012) and a Goh Cardiovascular Research Award (Duke-
570 NUS-GCR/2015/0014).

571 For the purpose of open access, the authors have applied a Creative Commons Attribution (CC
572 BY) licence to any Author Accepted Manuscript version arising.

573 Disclosures

574 SAC is a co-inventor on a number of patent applications relating to the role of IL11 in human
575 diseases that include the published patents: WO2017103108, WO2017103108 A2, WO
576 2018/109174 A2, WO 2018/109170 A2. SAC is also a co-founder and shareholder of Enleofen
577 Bio PTE LTD and VVB PTE LTD.

578 References

- 579 1. Paul SR, Bennett F, Calvetti JA, Kelleher K, Wood CR, O'Hara RM Jr, Leary AC,
580 Sibley B, Clark SC, Williams DA, et al. Molecular cloning of a cDNA encoding
581 interleukin 11, a stromal cell-derived lymphopoietic and hematopoietic cytokine. *Proc*
582 *Natl Acad Sci U S A*. 1990;87:7512–7516.
- 583 2. Neben TY, Loebelenz J, Hayes L, McCarthy K, Stoudemire J, Schaub R, Goldman SJ.
584 Recombinant human interleukin-11 stimulates megakaryocytopoiesis and increases
585 peripheral platelets in normal and splenectomized mice. *Blood*. 1993;81:901–908.
- 586 3. Zhang J-J, Zhao R, Xia F, Li Y, Wang R-W, Guan X, Zhu J-G, Ma A-X. Cost-
587 effectiveness analysis of rhTPO and rhIL-11 in the treatment of chemotherapy-induced
588 thrombocytopenia in hematological tumors based on real-world data. *Ann Palliat Med*.
589 2022;11:2709–2719.
- 590 4. Kaye JA. FDA licensure of NEUMEGA to prevent severe chemotherapy-induced
591 thrombocytopenia. *Stem Cells*. 1998;16 Suppl 2:207–223.
- 592 5. Yu K-M, Lau JY-N, Fok M, Yeung Y-K, Fok S-P, Zhang S, Ye P, Zhang K, Li X, Li J,
593 Xu Q, Wong W-T, Choo Q-L. Preclinical evaluation of the mono-PEGylated
594 recombinant human interleukin-11 in cynomolgus monkeys. *Toxicol Appl Pharmacol*.
595 2018;342:39–49.
- 596 6. Nakagawa M, Owada Y, Izumi Y, Nonin S, Sugioka K, Nakatani D, Iwata S, Mizutani
597 K, Nishimura S, Ito A, Fujita S, Daimon T, Sawa Y, Asakura M, Maeda M, Fujio Y,
598 Yoshiyama M. Four cases of investigational therapy with interleukin-11 against acute
599 myocardial infarction. *Heart Vessels*. 2016;31:1574–1578.
- 600 7. Nandurkar HH, Robb L, Tarlinton D, Barnett L, Köntgen F, Begley CG. Adult mice
601 with targeted mutation of the interleukin-11 receptor (IL11Ra) display normal
602 hematopoiesis. *Blood*. 1997;90:2148–2159.
- 603 8. Ng B, Widjaja AA, Viswanathan S, Dong J, Chothani SP, Lim S, Shekeran SG, Tan J,
604 McGregor NE, Walker EC, Sims NA, Schafer S, Cook SA. Similarities and differences
605 between IL11 and IL11RA1 knockout mice for lung fibro-inflammation, fertility and
606 craniosynostosis. *Sci Rep*. 2021;11:14088.
- 607 9. Tanaka M, Hirabayashi Y, Sekiguchi T, Inoue T, Katsuki M, Miyajima A. Targeted
608 disruption of oncostatin M receptor results in altered hematopoiesis. *Blood*.
609 2003;102:3154–3162.
- 610 10. Denton CP, Del Galdo F, Khanna D, Vonk MC, Chung L, Johnson SR, Varga J, Furst
611 DE, Temple J, Zecchin C, Csomor E, Lee A, Wisniacki N, Flint SM, Reid J. Biological
612 and clinical insights from a randomised phase II study of an anti-oncostatin M
613 monoclonal antibody in systemic sclerosis. *Rheumatology* [Internet]. 2022; Available
614 from: <http://dx.doi.org/10.1093/rheumatology/keac300>
- 615 11. Smith JW 2nd. Tolerability and side-effect profile of rhIL-11. *Oncology* . 2000;14:41–
616 47.

- 617 12. Liu N-W, Huang X, Liu S, Liu W-J, Wang H, Wang W, Lu Y. Elevated BNP caused by
618 recombinant human interleukin-11 treatment in patients with chemotherapy-induced
619 thrombocytopenia. *Support Care Cancer* [Internet]. 2019; Available from:
620 <http://dx.doi.org/10.1007/s00520-019-04734-z>
- 621 13. Obana M, Miyamoto K, Murasawa S, Iwakura T, Hayama A, Yamashita T, Shiragaki
622 M, Kumagai S, Miyawaki A, Takewaki K, Matsumiya G, Maeda M, Yoshiyama M,
623 Nakayama H, Fujio Y. Therapeutic administration of IL-11 exhibits the postconditioning
624 effects against ischemia-reperfusion injury via STAT3 in the heart. *Am J Physiol Heart*
625 *Circ Physiol*. 2012;303:H569-77.
- 626 14. Obana M, Maeda M, Takeda K, Hayama A, Mohri T, Yamashita T, Nakaoka Y,
627 Komuro I, Takeda K, Matsumiya G, Azuma J, Fujio Y. Therapeutic activation of signal
628 transducer and activator of transcription 3 by interleukin-11 ameliorates cardiac fibrosis
629 after myocardial infarction. *Circulation*. 2010;121:684–691.
- 630 15. Kimura R, Maeda M, Arita A, Oshima Y, Obana M, Ito T, Yamamoto Y, Mohri T,
631 Kishimoto T, Kawase I, Fujio Y, Azuma J. Identification of cardiac myocytes as the
632 target of interleukin 11, a cardioprotective cytokine. *Cytokine*. 2007;38:107–115.
- 633 16. Cook SA, Schafer S. Hiding in Plain Sight: Interleukin-11 Emerges as a Master
634 Regulator of Fibrosis, Tissue Integrity, and Stromal Inflammation. *Annu Rev Med*.
635 2020;71:263–276.
- 636 17. Corden B, Adami E, Sweeney M, Schafer S, Cook SA. IL-11 in cardiac and renal
637 fibrosis: Late to the party but a central player. *Br J Pharmacol*. 2020;177:1695–1708.
- 638 18. Sweeney M, O’Fee K, Villanueva-Hayes C, Rahman E, Lee M, Vanezis K, Andrew I,
639 Lim W-W, Widjaja A, Barton PJR, Cook SA. Cardiomyocyte-Restricted Expression of
640 IL11 Causes Cardiac Fibrosis, Inflammation, and Dysfunction. *Int J Mol Sci*.
641 2023;24:12989.
- 642 19. Ng B, Dong J, Viswanathan S, Widjaja AA, Paleja BS, Adami E, Ko NSJ, Wang M,
643 Lim S, Tan J, Chothani SP, Albani S, Schafer S, Cook SA. Fibroblast-specific IL11
644 signaling drives chronic inflammation in murine fibrotic lung disease. *FASEB J*.
645 2020;34:11802–11815.
- 646 20. Litviňuková M, Talavera-López C, Maatz H, Reichart D, Worth CL, Lindberg EL,
647 Kanda M, Polanski K, Heinig M, Lee M, Nadelmann ER, Roberts K, Tuck L, Fasouli
648 ES, DeLaughter DM, McDonough B, Wakimoto H, Gorham JM, Samari S, Mahbubani
649 KT, Saeb-Parsy K, Patone G, Boyle JJ, Zhang H, Zhang H, Viveiros A, Oudit GY,
650 Bayraktar OA, Seidman JG, Seidman CE, Nosedá M, Hubner N, Teichmann SA. Cells
651 of the adult human heart. *Nature*. 2020;588:466–472.
- 652 21. Litvinukova M, Lindberg E, Maatz H, Zhang H, Radke M, Gotthardt M, Saeb-Parsy K,
653 Teichmann S, Hübner N. Single cell and single nuclei analysis human heart tissue v1
654 [Internet]. 2018 [cited 2023 Aug 30]; Available from:
655 <https://www.protocols.io/view/single-cell-and-single-nuclei-analysis-human-heart-x54v98pkml3e/v1>
656
- 657 22. Sikkell MB, Francis DP, Howard J, Gordon F, Rowlands C, Peters NS, Lyon AR,

- 658 Harding SE, MacLeod KT. Hierarchical statistical techniques are necessary to draw
659 reliable conclusions from analysis of isolated cardiomyocyte studies. *Cardiovasc Res.*
660 2017;113:1743–1752.
- 661 23. Widjaja AA, Dong J, Adami E, Viswanathan S, Ng B, Pakkiri LS, Chothani SP, Singh
662 BK, Lim WW, Zhou J, Shekeran SG, Tan J, Lim SY, Goh J, Wang M, Holgate R, Hearn
663 A, Felkin LE, Yen PM, Dear JW, Drum CL, Schafer S, Cook SA. Redefining IL11 as a
664 regeneration-limiting hepatotoxin and therapeutic target in acetaminophen-induced liver
665 injury. *Sci Transl Med* [Internet]. 2021;13. Available from:
666 <http://dx.doi.org/10.1126/scitranslmed.aba8146>
- 667 24. Ahern BM, Levitan BM, Veeranki S, Shah M, Ali N, Sebastian A, Su W, Gong MC, Li
668 J, Stelzer JE, Andres DA, Satin J. Myocardial-restricted ablation of the GTPase RAD
669 results in a pro-adaptive heart response in mice. *J Biol Chem.* 2019;294:10913–10927.
- 670 25. Papa A, Zakharov SI, Katchman AN, Kushner JS, Chen B-X, Yang L, Liu G, Jimenez
671 AS, Eisert RJ, Bradshaw GA, Dun W, Ali SR, Rodrigues A, Zhou K, Topkara V, Yang
672 M, Morrow JP, Tsai EJ, Karlin A, Wan E, Kalocsay M, Pitt GS, Colecraft HM, Ben-
673 Johnny M, Marx SO. Rad regulation of CaV1.2 channels controls cardiac fight-or-flight
674 response. *Nat Cardiovasc Res.* 2022;1:1022–1038.
- 675 26. Ling SSM, Chen Y-T, Wang J, Richards AM, Liew OW. Ankyrin Repeat Domain 1
676 Protein: A Functionally Pleiotropic Protein with Cardiac Biomarker Potential. *Int J Mol*
677 *Sci* [Internet]. 2017;18. Available from: <http://dx.doi.org/10.3390/ijms18071362>
- 678 27. Zhang N, Ye F, Zhou Y, Zhu W, Xie C, Zheng H, Chen H, Chen J, Xie X. Cardiac
679 ankyrin repeat protein contributes to dilated cardiomyopathy and heart failure. *FASEB J.*
680 2021;35:e21488.
- 681 28. McCalmon SA, Desjardins DM, Ahmad S, Davidoff KS, Snyder CM, Sato K, Ohashi K,
682 Kielbasa OM, Mathew M, Ewen EP, Walsh K, Gavras H, Naya FJ. Modulation of
683 angiotensin II-mediated cardiac remodeling by the MEF2A target gene *Xirp2*. *Circ Res.*
684 2010;106:952–960.
- 685 29. Dewenter M, Pan J, Knödler L, Tzschöckel N, Henrich J, Cordero J, Dobрева G, Lutz S,
686 Backs J, Wieland T, Vettel C. Chronic isoprenaline/phenylephrine vs. exclusive
687 isoprenaline stimulation in mice: critical contribution of alpha1-adrenoceptors to early
688 cardiac stress responses. *Basic Res Cardiol.* 2022;117:15.
- 689 30. Schafer S, Viswanathan S, Widjaja AA, Lim W-W, Moreno-Moral A, DeLaughter DM,
690 Ng B, Patone G, Chow K, Khin E, Tan J, Chothani SP, Ye L, Rackham OJL, Ko NSJ,
691 Sahib NE, Pua CJ, Zhen NTG, Xie C, Wang M, Maatz H, Lim S, Saar K, Blachut S,
692 Petretto E, Schmidt S, Putoczki T, Guimarães-Camboia N, Wakimoto H, van Heesch S,
693 Sigmundsson K, Lim SL, Soon JL, Chao VTT, Chua YL, Tan TE, Evans SM, Loh YJ,
694 Jamal MH, Ong KK, Chua KC, Ong B-H, Chakaramakkil MJ, Seidman JG, Seidman
695 CE, Hubner N, Sin KYK, Cook SA. IL-11 is a crucial determinant of cardiovascular
696 fibrosis. *Nature.* 2017;552:110–115.
- 697 31. Stellato M, Dewenter M, Rudnik M, Hukara A, Özsoy Ç, Renoux F, Pachera E,
698 Gantenbein F, Seebeck P, Uhtjaerv S, Osto E, Razansky D, Klingel K, Henes J, Distler
699 O, Błyszczuk P, Kania G. The AP-1 transcription factor *Fosl-2* drives cardiac fibrosis

- 700 and arrhythmias under immunofibrotic conditions. *Commun Biol.* 2023;6:161.
- 701 32. van Duijvenboden K, de Bakker DEM, Man JCK, Janssen R, Günthel M, Hill MC,
702 Hooijkaas IB, van der Made I, van der Kraak PH, Vink A, Creemers EE, Martin JF,
703 Barnett P, Bakkers J, Christoffels VM. Conserved NPPB+ Border Zone Switches From
704 MEF2- to AP-1-Driven Gene Program. *Circulation.* 2019;140:864–879.
- 705 33. Agah R, Frenkel PA, French BA, Michael LH, Overbeek PA, Schneider MD. Gene
706 recombination in postmitotic cells. Targeted expression of Cre recombinase provokes
707 cardiac-restricted, site-specific rearrangement in adult ventricular muscle in vivo. *J Clin*
708 *Invest.* 1997;100:169–179.
- 709 34. Widjaja AA, Chothani S, Viswanathan S, Goh JWT, Lim W-W, Cook SA. IL11
710 Stimulates IL33 Expression and Proinflammatory Fibroblast Activation across Tissues.
711 *Int J Mol Sci* [Internet]. 2022;23. Available from:
712 <http://dx.doi.org/10.3390/ijms23168900>
- 713 35. Sartiani L, De Paoli P, Lonardo G, Pino R, Conti AA, Cerbai E, Pelleg A, Belardinelli L,
714 Mugelli A. Does recombinant human interleukin-11 exert direct electrophysiologic
715 effects on single human atrial myocytes? *J Cardiovasc Pharmacol.* 2002;39:425–434.
- 716 36. Xu J, Ren J-F, Mugelli A, Belardinelli L, Keith JC Jr, Pelleg A. Age-dependent atrial
717 remodeling induced by recombinant human interleukin-11: implications for atrial
718 flutter/fibrillation. *J Cardiovasc Pharmacol.* 2002;39:435–440.
- 719 37. Freire G, Ocampo C, Ilbawi N, Griffin AJ, Gupta M. Overt expression of AP-1 reduces
720 alpha myosin heavy chain expression and contributes to heart failure from chronic
721 volume overload. *J Mol Cell Cardiol.* 2007;43:465–478.
- 722 38. Beisaw A, Kuenne C, Guenther S, Dallmann J, Wu C-C, Bentsen M, Looso M, Stainier
723 DYR. AP-1 Contributes to Chromatin Accessibility to Promote Sarcomere Disassembly
724 and Cardiomyocyte Protrusion During Zebrafish Heart Regeneration. *Circ Res.*
725 2020;126:1760–1778.
- 726 39. Allanki S, Strilic B, Scheinberger L, Onderwater YL, Marks A, Günther S, Preussner J,
727 Kikhi K, Looso M, Stainier DYR, Reischauer S. Interleukin-11 signaling promotes
728 cellular reprogramming and limits fibrotic scarring during tissue regeneration. *Sci Adv.*
729 2021;7:eabg6497.
- 730 40. Cook SA. The Pathobiology of Interleukin 11 in Mammalian Disease is Likely
731 Explained by its Essential Evolutionary Role for Fin Regeneration. *J Cardiovasc Transl*
732 *Res* [Internet]. 2023; Available from: <http://dx.doi.org/10.1007/s12265-022-10351-9>
- 733 41. Dobin A, Davis CA, Schlesinger F, Drenkow J, Zaleski C, Jha S, Batut P, Chaisson M,
734 Gingeras TR. STAR: ultrafast universal RNA-seq aligner. *Bioinformatics.* 2013;29:15–
735 21.
- 736 42. Liao Y, Smyth GK, Shi W. featureCounts: an efficient general purpose program for
737 assigning sequence reads to genomic features. *Bioinformatics.* 2014;30:923–930.

- 738 43. Robinson MD, McCarthy DJ, Smyth GK. edgeR: a Bioconductor package for
739 differential expression analysis of digital gene expression data. *Bioinformatics*.
740 2010;26:139–140.
- 741 44. Mootha VK, Lindgren CM, Eriksson K-F, Subramanian A, Sihag S, Lehar J, Puigserver
742 P, Carlsson E, Ridderstråle M, Laurila E, Houstis N, Daly MJ, Patterson N, Mesirov JP,
743 Golub TR, Tamayo P, Spiegelman B, Lander ES, Hirschhorn JN, Altshuler D, Groop
744 LC. PGC-1alpha-responsive genes involved in oxidative phosphorylation are
745 coordinately downregulated in human diabetes. *Nat Genet*. 2003;34:267–273.
- 746 45. Subramanian A, Tamayo P, Mootha VK, Mukherjee S, Ebert BL, Gillette MA,
747 Paulovich A, Pomeroy SL, Golub TR, Lander ES, Mesirov JP. Gene set enrichment
748 analysis: a knowledge-based approach for interpreting genome-wide expression profiles.
749 *Proc Natl Acad Sci U S A*. 2005;102:15545–15550.
- 750 46. Kanehisa M, Goto S. KEGG: kyoto encyclopedia of genes and genomes. *Nucleic Acids*
751 *Res*. 2000;28:27–30.
- 752 47. Kanehisa M, Furumichi M, Sato Y, Kawashima M, Ishiguro-Watanabe M. KEGG for
753 taxonomy-based analysis of pathways and genomes. *Nucleic Acids Res*. 2023;51:D587–
754 D592.
- 755 48. Ge SX, Jung D, Yao R. ShinyGO: a graphical gene-set enrichment tool for animals and
756 plants. *Bioinformatics*. 2020;36:2628–2629.
- 757 49. Buenrostro JD, Giresi PG, Zaba LC, Chang HY, Greenleaf WJ. Transposition of native
758 chromatin for fast and sensitive epigenomic profiling of open chromatin, DNA-binding
759 proteins and nucleosome position. *Nat Methods*. 2013;10:1213–1218.
- 760 50. Corces MR, Trevino AE, Hamilton EG, Greenside PG, Sinnott-Armstrong NA, Vesuna
761 S, Satpathy AT, Rubin AJ, Montine KS, Wu B, Kathiria A, Cho SW, Mumbach MR,
762 Carter AC, Kasowski M, Orloff LA, Risca VI, Kundaje A, Khavari PA, Montine TJ,
763 Greenleaf WJ, Chang HY. An improved ATAC-seq protocol reduces background and
764 enables interrogation of frozen tissues. *Nat Methods*. 2017;14:959–962.